



HAL
open science

H3K4me1 Supports Memory-like NK Cells Induced by Systemic Inflammation

Orhan Rasid, Christine Chevalier, Tiphaine Marie-Noelle Camarasa,
Catherine Fitting, Jean-Marc Cavaillon, Melanie Anne Hamon

► **To cite this version:**

Orhan Rasid, Christine Chevalier, Tiphaine Marie-Noelle Camarasa, Catherine Fitting, Jean-Marc Cavaillon, et al.. H3K4me1 Supports Memory-like NK Cells Induced by Systemic Inflammation. Cell Reports, 2019, 29 (12), pp.3933-3945.e3. 10.1016/j.celrep.2019.11.043 . pasteur-03229812

HAL Id: pasteur-03229812

<https://pasteur.hal.science/pasteur-03229812>

Submitted on 19 May 2021

HAL is a multi-disciplinary open access archive for the deposit and dissemination of scientific research documents, whether they are published or not. The documents may come from teaching and research institutions in France or abroad, or from public or private research centers.

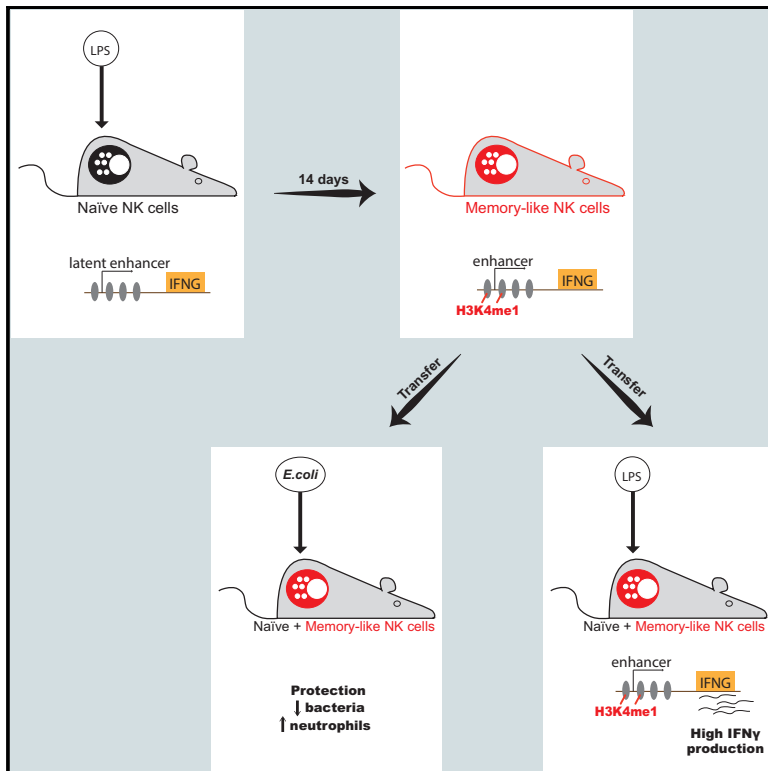
L'archive ouverte pluridisciplinaire **HAL**, est destinée au dépôt et à la diffusion de documents scientifiques de niveau recherche, publiés ou non, émanant des établissements d'enseignement et de recherche français ou étrangers, des laboratoires publics ou privés.



Distributed under a Creative Commons Attribution - NonCommercial - NoDerivatives 4.0 International License

H3K4me1 Supports Memory-like NK Cells Induced by Systemic Inflammation

Graphical Abstract



Authors

Orhan Rasid, Christine Chevalier, Tiphaine Marie-Noelle Camarasa, Catherine Fitting, Jean-Marc Cavillon, Melanie Anne Hamon

Correspondence

orhan.rasid@pasteur.fr (O.R.), melanie.hamon@pasteur.fr (M.A.H.)

In Brief

Rasid et al. show that sepsis-like systemic inflammation induces a type of long-lasting innate immune memory in NK cells, which can protect from *E. coli* infection. This is achieved by revealing an enhancer of IFN γ through histone monomethylation.

Highlights

- NK cells acquire cell-intrinsic memory-like properties after systemic inflammation
- Memory-like NK cells uncover a H3K4me1-marked enhancer at -22 kb of the *ifng* TSS
- Memory-like NK cells persist for 9 weeks and can protect from bacterial infection
- Memory-like and protective properties are methyltransferase dependent



H3K4me1 Supports Memory-like NK Cells Induced by Systemic Inflammation

Orhan Rasid,^{1,2,*} Christine Chevalier,¹ Tiphaine Marie-Noelle Camarasa,^{1,3} Catherine Fitting,² Jean-Marc Cavillon,² and Melanie Anne Hamon^{1,4,*}

¹G5 Chromatine et Infection, Institut Pasteur, Paris, France

²Unité Cytokines & Inflammation, Institut Pasteur, Paris, France

³Université Paris Diderot, Sorbonne Paris Cité, Paris, France

⁴Lead Contact

*Correspondence: orhan.rasid@pasteur.fr (O.R.), melanie.hamon@pasteur.fr (M.A.H.)

<https://doi.org/10.1016/j.celrep.2019.11.043>

SUMMARY

Natural killer (NK) cells are unique players in innate immunity and, as such, an attractive target for immunotherapy. NK cells display immune memory properties in certain models, but the long-term status of NK cells following systemic inflammation is unknown. Here we show that following LPS-induced endotoxemia in mice, NK cells acquire cell-intrinsic memory-like properties, showing increased production of IFN γ upon specific secondary stimulation. The NK cell memory response is detectable for at least 9 weeks and contributes to protection from *E. coli* infection upon adoptive transfer. Importantly, we reveal a mechanism essential for NK cell memory, whereby an H3K4me1-marked latent enhancer is uncovered at the *ifng* locus. Chemical inhibition of histone methyltransferase activity erases the enhancer and abolishes NK cell memory. Thus, NK cell memory develops after endotoxemia in a histone methylation-dependent manner, ensuring a heightened response to secondary stimulation.

INTRODUCTION

In recent years, accumulating evidence of memory responses mediated by innate immune cells has blurred the boundaries between innate and adaptive immunity (Netea et al., 2011; Sun et al., 2014). Monocytes and macrophages have been described to mediate a type of innate immune memory, termed trained immunity (Netea et al., 2016). Briefly, this refers to the long-lasting altered responsiveness of cells to a secondary stimulation, with either lower (tolerized) or higher (trained) inflammatory responses, involving chromatin modifications and metabolic rewiring (Saeed et al., 2014). Although trained immunity in phagocytes is always non-specific and results in a general hyper or hyporesponsiveness to re-stimulation, other innate cells, such as natural killer (NK) cells, can exhibit both non-specific memory-like features as well as a high degree of antigen specificity in a secondary response, depending on the model (Cerwenka and Lanier, 2016; Netea et al., 2016). NK cells have been shown to display memory-like properties to cytokine stimulation and anti-

gen-specific memory features to viral infection or hapten-induced contact hypersensitivity, but evidence of memory following bacterial infection remains scarce (Cerwenka and Lanier, 2016). The specificity of the recall response together with proliferation of specific receptor-defined sub-populations make NK cell memory more akin to classical adaptive memory mediated by T cells (Geary and Sun, 2017).

NK cell memory was demonstrated in several *in vivo* models of viral infection, particularly mouse cytomegalovirus (MCMV), in which the murine Ly49H receptor, specifically recognizing the MCMV m157 glycoprotein, defines a population of responsive NK cells that acquire memory (Sun et al., 2009). In humans infected with cytomegalovirus (CMV), the NKG2C receptor was involved in ensuring NK cell responses to specific viral peptides (Hammer et al., 2018). At the molecular level, NK cell memory to CMV has been correlated with modified chromatin states (Tesi et al., 2016). Mouse and human memory-like NK cells have modulated DNA methylation levels, which are notably reduced at the *ifng/IFNG* gene locus (Luetke-Eversloh et al., 2014), and more accessible chromatin at effector genes as assessed by ATAC-seq (Lau et al., 2018). However, whether these or other chromatin marks are important for establishing and maintaining memory remains to be determined.

Systemic inflammation, such as sepsis or severe trauma, represents one of the most complex paradigms in immunology and involves an overzealous inflammatory response that often represents a life-threatening condition (Cavillon et al., 2003). NK cells are among the main drivers of systemic inflammation during the acute phase, but afterward, they are severely incapacitated, similarly to monocytes and T cells (Chiche et al., 2011; Guo et al., 2018; Souza-Fonseca-Guimaraes et al., 2012a). Specifically, NK cells have impaired cytotoxicity and cytokine production in mouse models and human sepsis patients (Chiche et al., 2012; Souza-Fonseca-Guimaraes et al., 2012b, 2012c; von Muller et al., 2007). Altogether, these immune consequences are known as the “immunosuppressive” phase of systemic inflammation (Cavillon and Giamarellos-Bourboulis, 2019), a state of immune dysfunction that persists beyond the acute event, causing poor quality of life and increased susceptibility to infection (Shankar-Hari and Rubinfeld, 2016). However, although short-term consequences on the immune system are fairly well explored, the long-term status of NK cells after systemic inflammation remains to be explored and could have important implications, given their



well-known role as critical effectors in viral and bacterial infections (Vivier et al., 2008).

Herein, we used an endotoxemia model to explore the lasting impact of systemic inflammation on NK cells. We found that NK cells acquire cell-intrinsic memory-like properties, demonstrated by increased IFN γ production upon re-challenge, up to 9 weeks after endotoxemia. Strikingly, systemic inflammation reveals a latent enhancer at the *ifng* locus in memory-like NK cells, and blocking this, along with histone methylation, prevents acquisition of memory. Thus, we report that despite the suppressive immune environment that follows systemic inflammation, NK cells retain memory-like properties that are encoded at the chromatin level and help protect mice against bacterial infection.

RESULTS

NK Cells Are Responsive after Endotoxemia and Acquire Memory-like Properties despite Being in a Suppressive Environment

In order to assess the long-term effects of systemic inflammation on NK cells, we used an endotoxemia model (10 mg/kg lipopolysaccharide [LPS], intraperitoneal [i.p.]) causing acute inflammation but low mortality, with full clinical recovery by day 7 (Figures 1A–1C). Mice exhibited transient weight loss, clinical signs of inflammation, and limited mortality. Using this model, we had previously shown that NK cells are systemically activated over a 48 h acute period (Rasid et al., 2016). In the present study, we focused on the impact of endotoxemia on NK cells 14 days after LPS injection. First, we phenotypically defined NK cells at 14 days after endotoxemia (full gating strategy in Figure S1A). We found no significant differences in NK cell percentages or total numbers in the spleens of mice that received PBS injections as control (D14PBS) or experienced endotoxemia 14 days prior (D14LPS) (Figures 1D and 1E). Furthermore, although we found some variations in NK cell phenotype (Figures S1B–S1E), such differences did not correlate with an altered baseline of IFN γ expression detected upon *ex vivo* staining in D14LPS mice compared with D14PBS (Figure S1F). Together these data indicate that 14 days after endotoxemia, although NK cells acquire slight phenotypical differences, they return to a resting state, similar to that of naive cells.

We next tested the responsiveness of NK cells from post-endotoxemia mice *in vitro* both within the environment of the spleen and separately as purified cells. We first stimulated total spleen cells with LPS and observed significantly reduced IFN γ -positive NK cell percentages from D14LPS samples compared with D14PBS controls, as well as reduced total IFN γ in supernatants (Figures 1F–1H). In correlation with the lower levels of NK cell activation in D14LPS mice, we found a significant increase in percentages of regulatory T cells (Tregs) and accumulation of immature myeloid cells in these mice compared with D14PBS controls (Figure S2). Therefore, the immune environment in the spleen 14 days after systemic inflammation is suppressive and affects NK cells, which agrees with previous reports (Benjamin et al., 2005; Cavassani et al., 2010; Delano et al., 2007). Surprisingly, stimulation with IL-12+IL-18, targeted NK cell activators, induced similar levels of NK cell response between D14PBS and D14LPS splenocytes (Figures 1F–1H). These results sug-

gested that although post-endotoxemia spleen cells cannot activate NK cells in response to LPS, the intrinsic responsiveness of NK cells, at least to IL-12+IL-18, is not altered 14 days after endotoxemia.

To further study the response of NK cells independently of the splenic environment, we stimulated enriched NK cells (~80%) *in vitro*. We had previously shown that isolated NK cells respond to LPS stimulation *in vitro* if co-stimulated with the cytokines IL-15+IL-18, which do not induce sustained activation on their own (Souza-Fonseca-Guimaraes et al., 2012b). In agreement, whereas overnight stimulation with IL-15+IL-18 induced no detectable response, IL-12+IL-18 stimulation induced sustained IFN γ production. However, no differences were observed between control D14PBS and D14LPS NK cells in terms of IFN γ + percentages or total IFN γ production in supernatants (Figures 1I–1K), as we had observed when stimulating total spleen cells. We also found no differences in the expression levels of various cytokine receptors on NK cells from D14PBS or LPS mice (Figure S3A). To exclude an effect of saturation level stimulation, we titrated down IL-12+IL-18 and still observed no significant difference in responsiveness between D14PBS or D14LPS NK cells (Figure S3B). Stimulation with plate-bound antibodies against various NK cell receptors also revealed no differences (Figure S3C). In contrast, upon stimulation with IL-15+IL-18+LPS, we found that D14LPS NK cells had significantly higher percentages of IFN γ + cells compared with control D14PBS NK cells (Figures 1I and 1J). The higher responsiveness of D14LPS NK cells was confirmed by measuring total levels of secreted IFN γ , as well as granulocyte-macrophage colony-stimulating factor (GM-CSF), in cell culture supernatants (Figures 1K and 1L). Other cytokines tested but undetected were TNF, IL-6, IL-10, and CCL3 and CCL4 (data not shown). Altogether, these results indicate that following systemic inflammation, NK cells have a significantly increased responsiveness to LPS *in vitro*, a memory-like property.

Because our *in vitro* stimulations are performed on enriched NK cells, we cannot exclude a possible effect of contaminants such as myeloid or T cells. To exclude this possibility, we performed the same experiments as above but mixed enriched (~80%) naive CD45.1 NK cells with CD45.2 D14PBS or D14LPS NK cells, which were highly purified (~98%). In this way, each well containing D14PBS or D14LPS NK cells has an internal control of naive NK cells, which are subjected to the same influence of possible contaminants. Cocultured naive and D14PBS NK cells responded similarly to IL-15+IL-18+LPS stimulation, as expected (Figures S3D and S3E). Furthermore, naive cells cocultured with D14LPS NK cells reached slightly higher levels of IFN γ expression compared with D14PBS NK cells, but these were significantly surpassed by the cocultured D14LPS NK cells (Figures S3D and S3E). Therefore, these results strongly support cell-intrinsic memory-like responses observed in D14LPS NK cells. Notably, the unaltered production of IFN γ in response to cytokine stimulation suggests that changes in NK cell reactivity after endotoxemia do not simply reflect a state of hyperresponsiveness. Altogether, our results show that 2 weeks post-endotoxemia, NK cells are responsive and have acquired cell-intrinsic memory-like properties, even though these are in a suppressive environment.

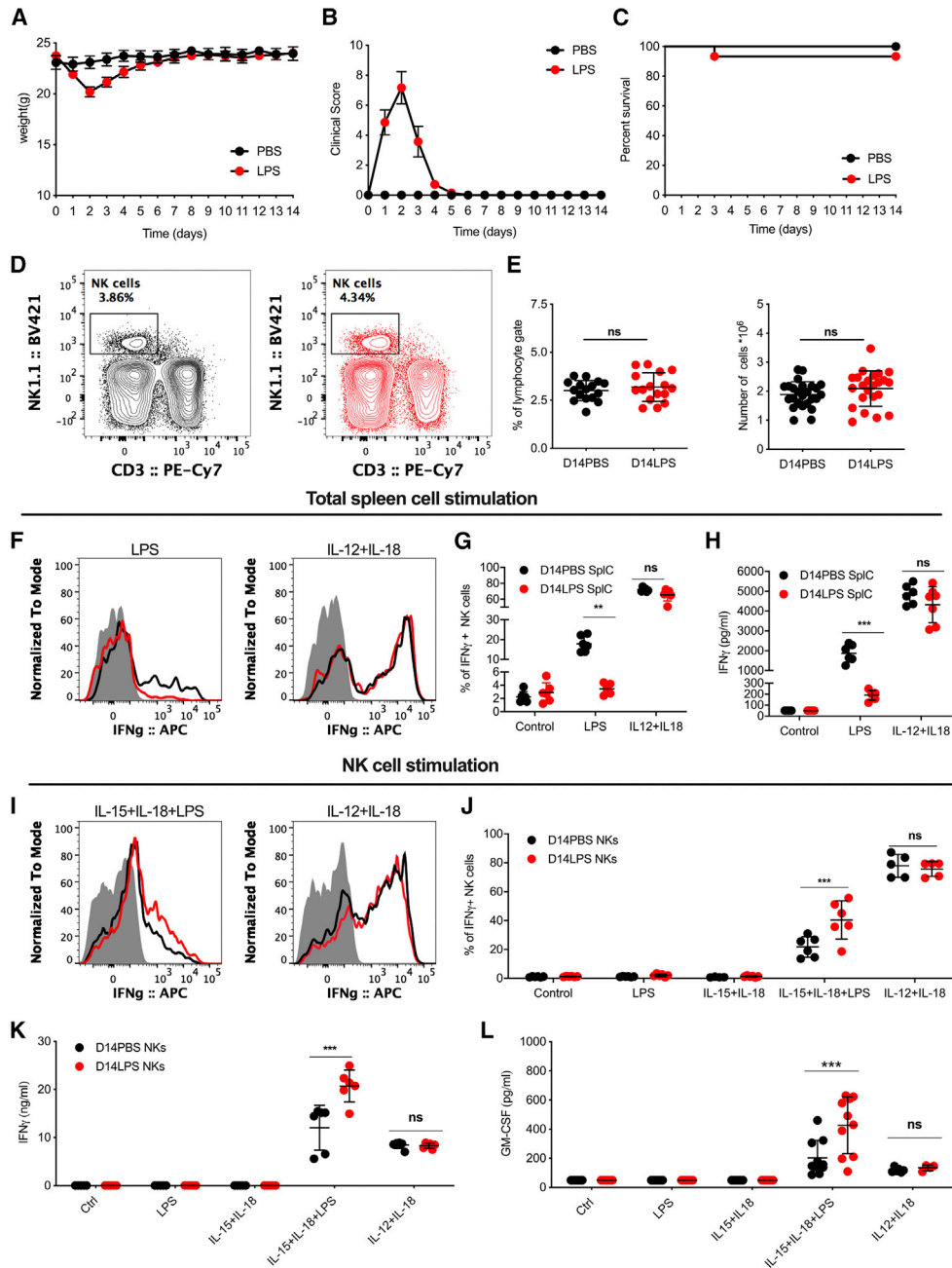


Figure 1. NK Cells Acquire Memory-like Features 14 Days after Endotoxemia

C57BL/6 mice were injected with either PBS (black symbols and lines) or LPS (10 mg/kg) (red symbols and lines) intraperitoneally and monitored for 14 day, after which they were used to assess NK cell status *ex vivo*.

(A–C) Weight (A), clinical score (B), and survival monitoring (C) following injection of PBS or LPS.

(D and E) Spleen NK cells from D14PBS and D14LPS mice were analyzed: (D) representative gating for NK cells in both conditions and (E) percentages of NK cells among lymphocytes and total NK cell numbers. Splenocytes (SpIC) from D14PBS and LPS mice were stimulated *in vitro* with cytokines (10 ng/mL) or LPS (100 ng/mL) overnight. Cells were stained for flow cytometry analysis to assess levels of intracellular IFN γ , and supernatants were collected for cytokine ELISAs. (F and G) Representative overlay histograms (gray represents isotype control) (F) and quantification (G) of IFN γ expression by NK cells in respective conditions. (H) Total IFN γ levels in supernatants from SpIC. NK cells were enriched from spleens of D14PBS and LPS mice and stimulated *in vitro* with cytokines and/or LPS overnight.

(I and J) Representative overlay histograms (gray represents isotype control) (I) and quantification (J) of IFN γ expression by NK cells in respective conditions. (K and L) Total (K) IFN γ and (L) GM-CSF levels in supernatants from NK cells in respective conditions.

Dots represent individual mice. Data represent one of at least three repeats with $n \geq 5$ mice/group. ns, not significant. ** $p < 0.01$ and *** $p < 0.001$, Mann-Whitney test comparing D14PBS and D14LPS cell values.

Endotoxemia-Induced Memory-like NK Cells Are Detectable *In Vivo*

We further explored the memory responses of NK cells *in vivo* upon LPS challenge. In order to compare D14LPS NK cells with naive counterparts in the same immune environment, we used an adoptive transfer model in which naive congenic NK cells were transferred into post-endotoxemic mice (Figure 2A). We transferred naive CD45.1 NK cells into CD45.2 mice that had been treated with PBS or LPS 13 days prior. On day 14, recipient mice were re-challenged with PBS or LPS, and NK cell responses in the spleen were assessed 6 h later. Transferred naive NK cells were readily identified by CD45.1 staining, and their IFN γ expression was quantifiable (Figure 2B). Importantly, control PBS injection induced no detectable IFN γ in either the endogenous or transferred NK cell populations, further demonstrating that 14 days after endotoxemia, NK have returned to a resting state (Figure 2C). LPS re-challenge induced significant expression of IFN γ by endogenous NK cells as well as transferred naive NK cells in D14PBS mice (Figure 2D, left). Because both endogenous and transferred NK cells responded at similar levels, the transfer procedure itself had no influence on IFN γ response. In D14LPS mice, the percentages of IFN γ + NK cells were significantly lower compared with those from D14PBS mice (Figure 2D), as expected given the suppressive environment we described for the spleen. Strikingly, endogenous D14LPS NK cells had significantly higher percentages of IFN γ + cells than transferred naive NK cells (Figure 2D, right). These results demonstrate that acquisition of NK cell memory-like features after systemic inflammation results in increased responsiveness to re-stimulation *in vivo* even in the post-endotoxemic suppressive environment.

The Ly49H and NKG2C receptors have both been implicated in mediating NK cell memory responses to MCMV and CMV, respectively (Lopez-Vergès et al., 2011; Sun et al., 2009), and we observed differences in NK cell sub-populations defined by these receptors after endotoxemia (Figure S1C). We thus investigated whether these sub-populations might be involved in mediating memory in our model. We compared populations defined by NKG2A/C/E and Ly49H in both D14PBS and D14LPS mice and found no difference in the percentages of IFN γ + cells upon LPS re-challenge between positive or negative populations (Figures S4A and S4B). These results suggest that neither of these sub-populations is involved in the observed results; thus, we conducted the rest of our study using the bulk NK cell population.

To explore memory NK cell function independently of the surrounding immunological environment, we turned to another adoptive transfer system in which we evaluate intrinsic NK cell properties. We transferred D13PBS or D13LPS NK cells into naive congenic mice 1 day before re-challenge with PBS or LPS (Figure 2E). Thus, CD45.2 D14PBS or D14LPS NK cells were compared with naive endogenous CD45.1 NK cells 6 h after PBS or LPS challenge (Figure 2F). PBS injection revealed no differences in basal IFN γ expression between transferred CD45.2 and endogenous naive CD45.1 NK cells, suggesting that both D14PBS and D14LPS NK cells remain in a resting state even outside the suppressive environment of the post-endotoxemia spleen (Figure 2G). Upon LPS injection, a high per-

centage of IFN γ + cells are detected in both control transferred D14PBS NK cells and endogenous naive NK cells (Figure 2H, left). Strikingly, significantly higher percentages of IFN γ + cells were detected in the transferred D14LPS NK cells compared with the respective endogenous NK cells (Figure 2H, right). These results firmly demonstrate that NK cells intrinsically acquire memory-like features 14 days following systemic inflammation, and this is independent of the surrounding immune environment.

Endotoxemia-Induced Memory-like NK Cells Persists for at Least 9 Weeks

The lasting potential is an important feature of a memory response, which we explored 9 weeks after endotoxemia. We tested the responsiveness of NK cells by performing adoptive transfer schemes similar to those in Figures 2A and 2E but 9 weeks after PBS or LPS injection (We9PBS/LPS). Remarkably, memory-like properties of NK cells were retained at this moment. Indeed, endogenous We9LPS NK cells responded with more IFN γ than transferred naive NK cells, despite the suppressive environment, which was still present at this time (Figure 3A), albeit less restrictive than at day 14. Additionally, transferred We9LPS NK cells still surpassed endogenous NK cells in IFN γ + percentages in naive recipient mice (Figure 3B). We also performed *in vitro* stimulations of enriched NK cells and observed that We9LPS NK cells were still significantly more responsive to IL-15+IL-18+LPS than We9PBS NK cells (Figures 3C and 3D). Therefore, post-endotoxemia NK cells retain memory-like properties, characterized by an increased IFN γ production to LPS challenge, a memory-like state that persists for at least 9 weeks.

Memory-like Cells Derive from NK Cells that Experienced Endotoxemia

To investigate the origin of D14LPS NK cells and whether these cells are the same cells present at the time of endotoxemia, descendants of those cells, or new cells that migrated to the spleen after systemic inflammation, we made use of the adoptive transfer system described in Figure 4A. In this system, traceable congenic NK cells are transferred into recipient mice 1 day prior to endotoxemia and are followed through day 14. An additional transfer of naive NK cells is performed 7 days after endotoxemia in order to have control naive cells at day 14 in the same recipient mouse. Thus, we have a model in which a defined population of pre-transferred CD45.1 NK cells will have been exposed to the same control (D14PBS) or inflammatory (D14LPS) conditions as the endogenous CD45.1/2 NK cells, and a post-transferred population of naive CD45.2 NK cells that will serve as additional naive controls. Using this model, we re-challenged D14PBS and D14LPS CD45.1/2 mice with PBS or LPS and assessed IFN γ expression in NK cells. Because of the time period between the pre-transfer and the response readout, and the potential for NK cells plasticity into type 1 innate lymphoid cells (ILC1s) (Gao et al., 2017), we increased the stringency of our gating strategy for NK cells. We introduced an additional marker to our panel and defined our NK cells as CD3⁻NK1.1⁺CD49b⁺ (Figure 4B), thereby excluding interference of ILC1s. Pre-transferred CD45.1 and post-transferred CD45.2

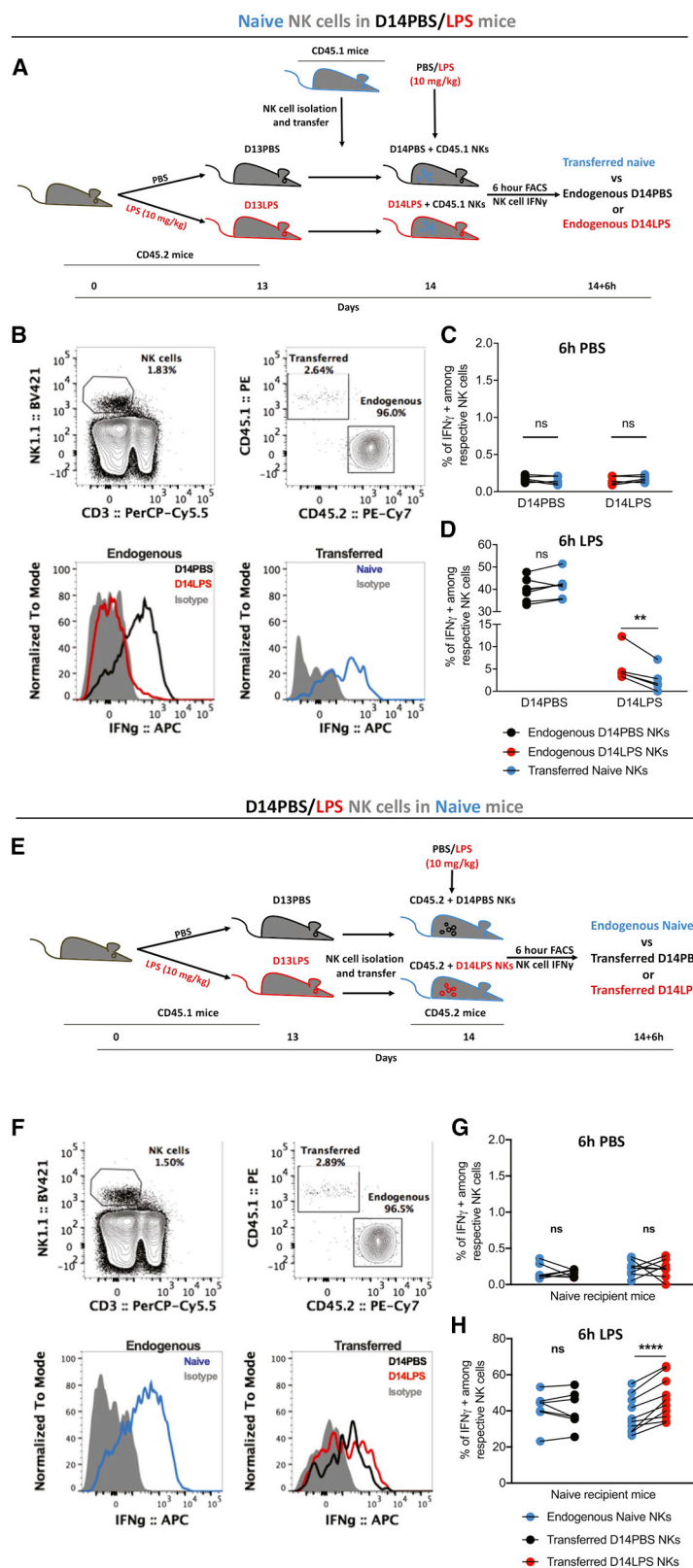


Figure 2. NK Cells Retain Cell-Intrinsic Memory Properties *In Vivo* after Endotoxemia Under a Suppressive Environment

NK cells enriched from spleens of naive CD45.1 mice were transferred into CD45.2 mice (1×10^6 cells/recipient, intravenously) injected 13 days before with PBS (D13PBS) (black) or LPS (10 mg/kg, i.p.) (D13LPS) (red). Recipient mice were challenged 1 day later with PBS or LPS (10 mg/kg) and sacrificed 6 h later. Splenocytes were processed for flow cytometry to evaluate levels of intracellular IFN γ in endogenous versus transferred NK cells.

(A) Experimental transfer scheme.

(B) Representative gating strategy for endogenous and transferred NKs (up) and overlay histograms for IFN γ + in respective subpopulations (down).

(C and D) Data summary: grouped before-after plots depicting percentages of IFN γ + cells among endogenous CD45.2 D14PBS NK cells (black dots), transferred CD45.1 naive NK cells (blue dots), and endogenous CD45.2 D14LPS NK cells (red dots) at 6 h after (C) PBS or (D) LPS re-challenge. NK cells were enriched from spleens of CD45.1 mice injected 13 days before with PBS (D13PBS) or LPS (10 mg/kg, i.p.) (D13LPS) and were transferred into naive CD45.2 mice (1×10^6 cells/recipient, intravenously). Recipient mice were challenged and samples harvested as above.

(E) Experimental transfer scheme.

(F) Representative gating strategy for endogenous and transferred NKs (up) and overlay histograms for IFN γ + in respective subpopulations (down).

(G and H) Data summary: grouped before-after plots depicting percentages of IFN γ + cells among endogenous CD45.2 naive NK cells (blue dots), transferred D14PBS CD45.1 NK cells (black dots), and transferred D14LPS CD45.2 NK cells (red dots) at 6 h after (G) PBS or (H) LPS re-challenge.

Dots represent individual mice. Data are representative of one experiment of three repeats with $n \geq 5$ mice/group. ns, not significant. ** $p < 0.01$ and **** $p < 0.0001$, Wilcoxon paired test comparing D14PBS, D14LPS, and naive cell values under respective condition.

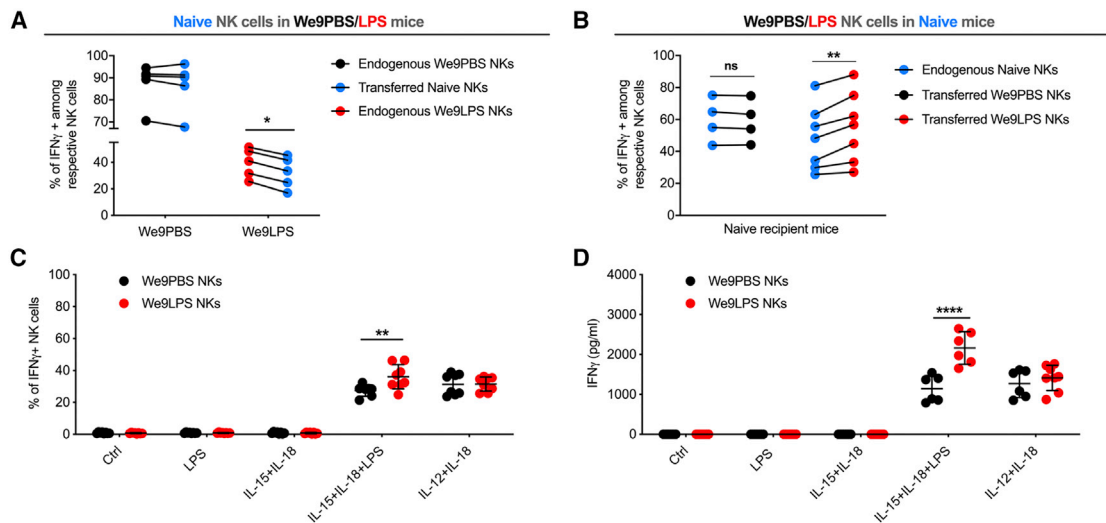


Figure 3. NK Cells Retain Memory Properties for at Least 9 Weeks after Endotoxemia

NK cells enriched from spleens of naive mice were transferred into congenic mice (1×10^6 cells/recipient, intravenously) injected 9 weeks before with PBS (We9PBS) or LPS (10 mg/kg, i.p.) (We9LPS). Recipient mice were challenged 1 day later with LPS (10 mg/kg) and sacrificed 6 h later. Splenocytes were processed for flow cytometry to evaluate levels of intracellular $\text{IFN}\gamma$ in endogenous versus transferred NK cells.

(A) Data summary: grouped before-after plots depicting percentages of $\text{IFN}\gamma^+$ cells among endogenous We9PBS NK cells (black dots), transferred naive NK cells (blue dots), and endogenous We9LPS NK cells (red dots) at 6 h after LPS re-challenge. NK cells were enriched from spleens of mice injected 9 weeks before with PBS (We9PBS) or LPS (10 mg/kg, i.p.) (We9LPS) and were transferred into naive congenic mice (1×10^6 cells/recipient, intravenously). Recipient mice were challenged and samples harvested as above.

(B) Data summary: grouped before-after plots depicting percentages of $\text{IFN}\gamma^+$ cells among endogenous naive NK cells (blue dots), transferred We9PBS NK cells (black dots), and transferred We9LPS NK cells (red dots) at 6 h after LPS re-challenge. NK cells were enriched from spleens of We9PBS and LPS mice and stimulated *in vitro* with cytokines (10 ng/mL) or LPS (100 ng/mL) overnight.

(C and D) Quantification of (C) $\text{IFN}\gamma$ expression by NK cells and total levels of (D) $\text{IFN}\gamma$ in respective conditions.

Dots represent individual mice. Data are representative of one experiment of three repeats with $n \geq 4$ mice/group. ns, not significant. * $p < 0.05$, ** $p < 0.01$, and **** $p < 0.0001$, Wilcoxon paired test comparing D14PBS, D14LPS, and naive cell values under respective conditions (A and B) and Mann-Whitney test comparing D14PBS and D14LPS values (C and D).

NK cells were readily detectable. Upon PBS injection, we observed no difference in basal $\text{IFN}\gamma$ expression by any NK cell population in D14PBS or LPS mice (Figure 4C). Furthermore, upon LPS injection into D14PBS mice, we observed similar percentages of $\text{IFN}\gamma^+$ cells among the pre-transferred D14PBS CD45.1, endogenous CD45.1/2 D14PBS, and post-transferred naive CD45.2 NK cell populations (Figure 4D, left; Figure S4C), demonstrating that in the absence of prior inflammation, transferred and endogenous cell populations behave similarly. However, upon LPS injection into D14LPS mice, we observe an increase in percentages of $\text{IFN}\gamma^+$ cells in endogenous D14LPS CD45.1/2 NK cells compared with post-transferred naive CD45.2 NK cells (Figure 4D, right; Figure S4D). Most interestingly, the pre-transferred D14LPS CD45.1 NK cells also showed significantly higher $\text{IFN}\gamma^+$ percentages compared with post-transferred naive CD45.2 NK cells and similar levels to endogenous cells (Figure 4D, right). This transfer system was also the ideal approach to address the involvement of NK cell-intrinsic TLR signaling in our endotoxemia model. Indeed, *in vitro* testing is hampered by the fact that a chronic lack of tonic TLR signaling lowers NK cell responsiveness in general (Ganal et al., 2012). By pre-transferring TLR2/4KO NK cells, we found that both primary and memory responses of NK cells during LPS challenge were independent of TLR2 and 4 (Figure S4E). Altogether, these results

demonstrate that NK cells present at the moment of systemic inflammation, or descendants of the original cells, acquire memory-like properties after endotoxemia, in a TLR2- and TLR4-independent manner.

To determine whether the endotoxemia-induced memory cells have proliferated during the course of 14 days, we pre-transferred CFSE-labeled CD45.1 NK cells into CD45.2 mice followed by PBS/LPS injection (Figure 4E). At day 14, in D14PBS mice we observed minimal CFSE dilution of pre-transferred NK cells (Figures 4F and 4G). In contrast, in D14LPS mice, the majority of pre-transferred NK had divided as indicated by several peaks of decreasing CFSE signal (Figures 4F and 4G). Our results thus demonstrate that D14LPS memory-like cells derive from NK cells that were exposed to systemic inflammation and maintain memory-like properties after undergoing several rounds of proliferation.

Histone Methylation at an *ifng* Enhancer Is Necessary for Memory-like NK Cells

Because innate immune memory in macrophages and NK cells has been proposed to rely on chromatin modifications, we explored whether this might be the case for post-endotoxemia memory-like NK cells. We assessed histone marks associated with upstream regulatory regions of the *ifng* locus by chromatin

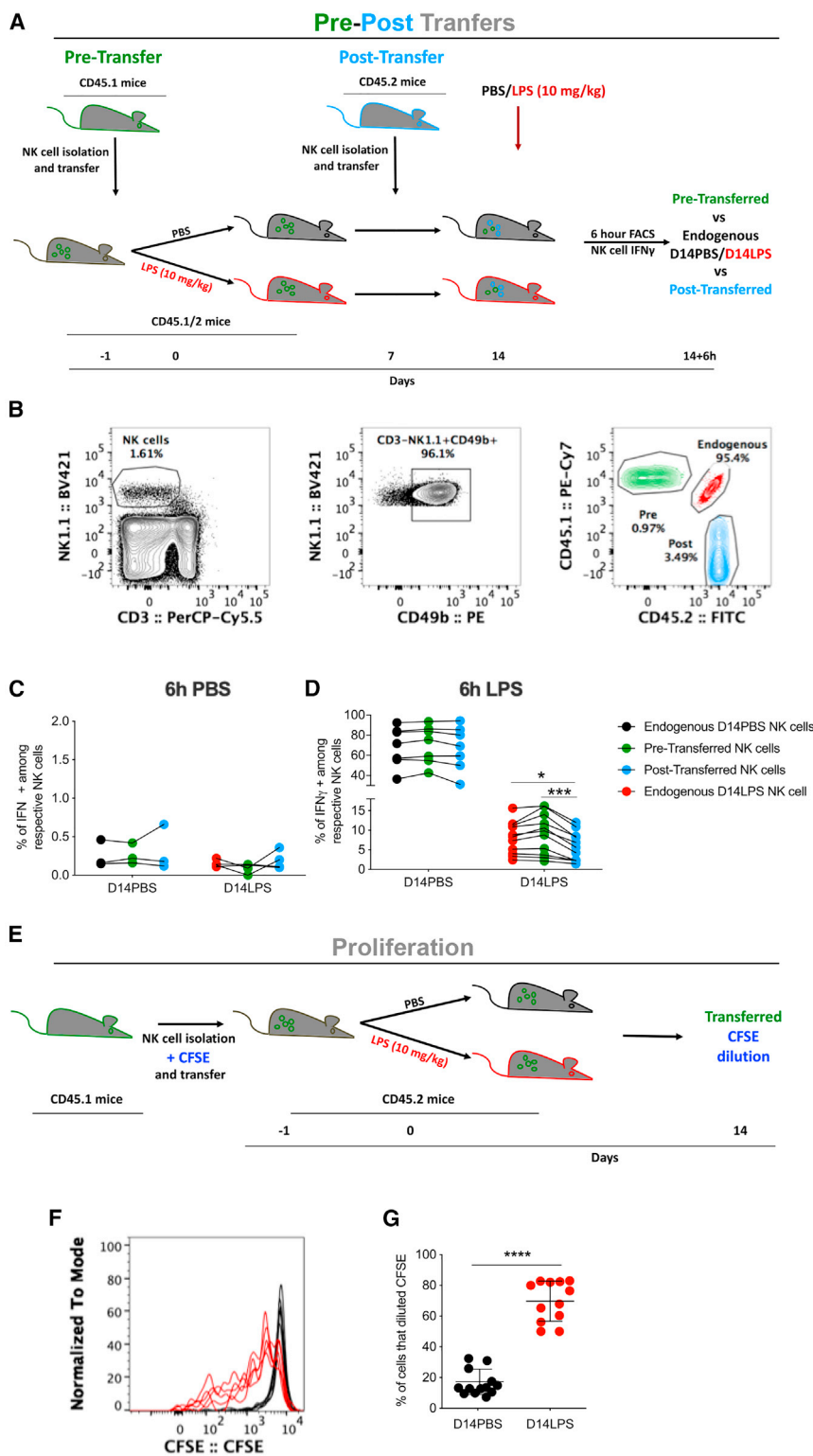


Figure 4. Memory-like Cells Derive from NK Cells that Experienced Endotoxemia

NK cells enriched from spleens of naive CD45.1 mice were pre-transferred into CD45.1/2 mice (1×10^6 cells/recipient, intravenously), 1 day before recipients were injected with PBS or LPS (10 mg/kg, i.p.). Naive CD45.2 enriched NK cells were post-transferred into the CD45.1/2 mice, 7 days after PBS/LPS injection. On day 14, mice were re-challenged with PBS/LPS and sacrificed 6 h later to assess intracellular IFN γ levels in endogenous, pre- and post-transferred NK cells.

(A) Experimental transfer scheme.

(B) Representative gating strategy.

(C and D) Data summary: before-after plots depicting percentages of IFN γ + cells among endogenous CD45.1/2 D14PBS NK cells (black dots), pre-transferred CD45.1 NK cells (green dots), post-transferred CD45.2 (blue dots), and endogenous CD45.1/2 D14LPS NK cells (red dots) at 6 h after (C) PBS or (D) LPS re-challenge. Enriched CD45.1 naive NK cells were labeled with CFSE and transferred into CD45.2 mice 1 day before PBS or LPS (10 mg/kg, i.p.) injection. On day 14, spleens were harvested from D14PBS and D14LPS mice and stained for transferred NK cell identification in order to assess CFSE dilution.

(E) Experimental transfer scheme.

(F) Representative overlay histogram showing CFSE dilution of CD45.1 transferred cells in D14PBS (black lines) and D14LPS (red lines) mice. (G) Data summary showing percentages of cells that diluted CFSE (gated on all cells before the highest intensity peak).

Dots represent individual mice. Data are representative of one experiment of three repeats with $n \geq 5$ mice/group. ns, not significant. * $p < 0.05$, *** $p < 0.001$, and **** $p < 0.0001$, Wilcoxon paired test comparing pre-transferred, post-transferred, and endogenous D14PBS, D14LPS, or naive cell values under respective conditions (C and D) and Mann-Whitney test comparing D14PBS and D14LPS values (G).

immunoprecipitation followed by qPCR (ChIP-qPCR). We probed the *ifng* promoter and several possible enhancer regions, which had been previously described as being crucial for IFN γ transcription (Figure 5A) (Balasubramani et al., 2014; Hatton

et al., 2006). As positive and negative controls, we probed ActB, a housekeeping gene known to be expressed and Hoxc8, that is silent in hematopoietic cells, respectively (Figure S5A). We focused on H3K4me1, a histone modification

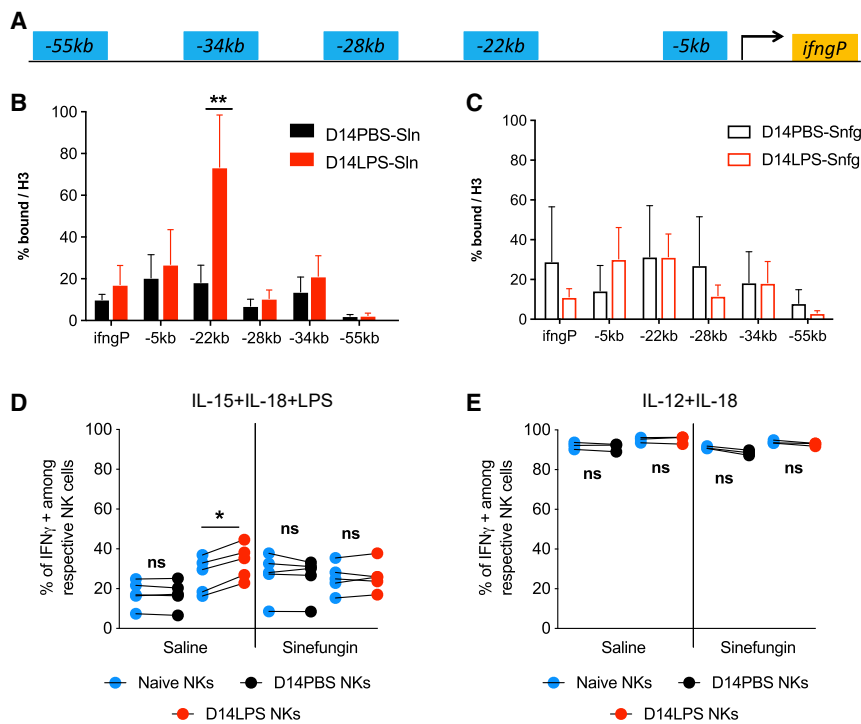


Figure 5. Histone Methylation Maintains NK Cell Memory after Endotoxemia

NK cells were isolated from spleens of mice injected 14 days before with PBS (D14PBS) or LPS (10 mg/kg, i.p.) (D14LPS) and treated with saline (Sln) or sinefungin (Snfgn) (10 mg/kg, i.p.) 2 days after PBS/LPS injection. Highly purified NK cells (3×10^6 to 6×10^6) were fixed, and chromatin was extracted and sheared. ChIP for H3K4me1 was performed, and resulting positive and H3 fractions of the chromatin were amplified using PCR for the indicated targets.

(A) Scheme of the *ifng* locus and known enhancers adapted from Balasubramani et al. (2014).

(B) Enrichment percentage for H3K4me1 pull-down on different regions of the *ifng* locus in NK cells from D14PBS/LPS mice treated with saline.

(C) Enrichment percentage for H3K4me1 pull-down on different regions of the *ifng* locus in NK cells from D14PBS/LPS mice treated with sinefungin. Mice were treated as above. On day 14, NK cells were highly purified from D14PBS or D14LPS mice that were treated with saline or sinefungin. NK cells from each group were mixed with enriched naive congenic NK cells and stimulated overnight in the indicated conditions (above graphs). Cells were stained for flow cytometry analysis of intracellular IFN γ levels in respective sub-populations.

(D and E) Data summary: grouped before-after plots depicting percentages of IFN γ + cells among

naive (blue dots), D14PBS (black dots), and D14LPS (red dots) NK cells stimulated with (D) IL-15+IL-18+LPS and (E) IL-12+IL-18. Treatment groups underneath graph.

Data are representative of one experiment of at least three repeats with $n \geq 3$ mice/group. ns, not significant. * $p < 0.05$ and ** $p < 0.01$, Mann-Whitney test (B and C) and Wilcoxon paired test (D and E) comparing D14PBS, D14LPS, and naive cell values under respective conditions.

that marks enhancers. Interestingly, we identified one region of the *ifng* locus, located -22 kb from the transcriptional start site, that showed significant enrichment for H3K4me1 in D14LPS NK cells (Figure 5B). The same region was not marked with H3K4me1 in D14PBS NK cells. We also looked at the levels of inhibitory and activatory marks, H3K27me3, H3K27ac, and H3K4me3, respectively, and found no significant differences in H3K27me3, H4K4me3, or H3K27ac at this region between D14PBS NK and D14LPS NK cells (Figures S5B–S5G). We further determined the levels of H3K4me1 9 weeks after endotoxemia. Remarkably, we observed a similar trend in enrichment for H3K4me1, without reaching significance, at this late time point (Figure S5H). Therefore, endotoxemia reveals a latent enhancer at the *ifng* locus, thereby poisoning NK cells for increased IFN γ expression. Such results strongly suggest that the development of post-endotoxemia memory-like NK cells is encoded in histone modifications.

To test the involvement of histone methylation on memory acquisition by NK cells after endotoxemia, we used a chemical methyltransferase inhibitor, sinefungin (Snfg), previously reported to reduce H3K4me1 *in vivo* (Sasaki et al., 2016). We treated mice with sinefungin or saline, as a vehicle control, 2 days after PBS or LPS injection. We performed ChIP-qPCR on NK cells from the respective groups of mice and found that sinefungin treatment blocked H3K4 monomethylation at the -22 kb enhancer in D14LPS-sinefungin mice (Figure 5C). At day 14,

we purified NK cells from the four groups of mice (D14PBS-saline, D14PBS-sinefungin, D14LPS-saline, and D14LPS-sinefungin) and stimulated them with IL15+IL18+LPS in co-culture with congenic naive NK cells. We observed no differences in control conditions (Figure S5I). Strikingly, whereas saline-treated D14LPS NK cells showed memory-like level responses, with higher IFN γ + percentages, compared with the co-cultured naive NK cells and D14PBS NK cells, sinefungin-treated D14LPS NK cells lost memory-like properties, responding at similar levels to co-cultured naive NK cells (Figure 5D). Similar results were observed when selectively gating strictly on conventional (CD49b+) NK cells (Figure S5J). Importantly, sinefungin treatment did not block the response of D14PBS or D14LPS NK cells to IL-12+IL-18 (Figure 5E). These results demonstrate that methyltransferase-dependent modifications in D14LPS NK cells are indeed acquired *de novo* and influence only the memory-like responses (IL-15+IL-18+LPS) and not the naive-level response to cytokines IL-12+IL-18 of D14LPS NK cells. Therefore, acquisition of NK cell memory-like properties following endotoxemia is mediated by a histone methylation-dependent mechanism, which reveals at least one latent enhancer at the *ifng* locus.

Memory-like NK Cells Contribute to Protection against Bacterial Infection

To investigate the potential role of endotoxemia-induced memory NK cells in the context of bacterial infection, we transferred 1×10^5

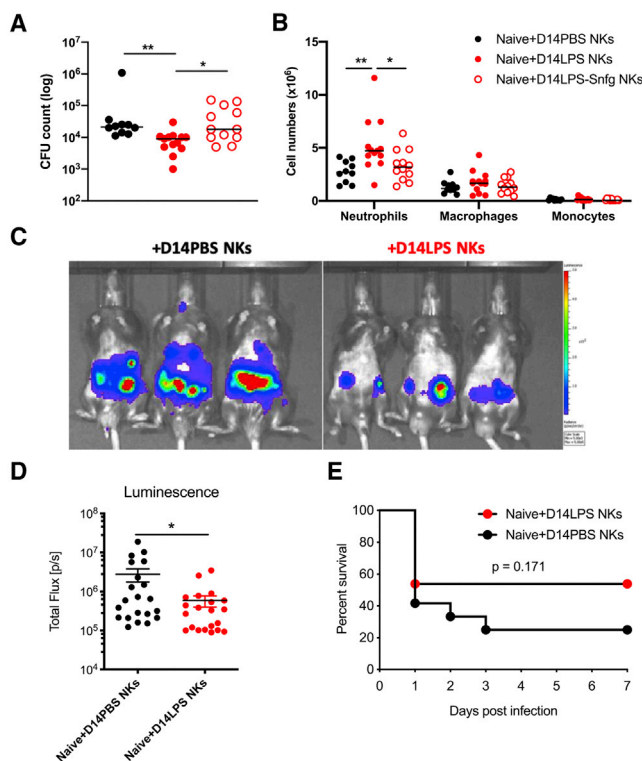


Figure 6. Memory NK Cells Protect from Bacterial Infection

NK cells purified from spleens of mice that were injected 14 days before with PBS (D14PBS) or LPS (10 mg/kg, i.p.) and one group treated with sinefungin (10 mg/kg, i.p.) (D14LPS and D14LPS-Snfg, respectively) were transferred into naive mice (1×10^5 cells/recipient, intravenously). Recipient mice were challenged 2 days later with luminescent *E. coli* (2×10^7 colony-forming units [CFU]/mouse) via intraperitoneal injection. Peritoneal lavages were harvested on day 1 post-infection for CFU counts and cellular infiltrate determination by flow cytometry.

(A) CFU counts in peritoneal lavages.

(B) Cellular infiltrate numbers for neutrophils (CD11b⁺Ly6G⁺Ly6C^{mid}), macrophages (CD11b⁺Ly6G⁻Ly6C^{neg/mid}CD64⁺), and monocytes (CD11b⁺Ly6G⁻Ly6C^{high}CD64⁻) in the infected mice. Luminescent images were acquired at day 1 post-infection, and survival was monitored for 7 days.

(C) Representative images of bacterial luminescent signal in challenged mice at day 1.

(D) Quantification of luminescent signal.

(E) Kaplan-Meier survival curve for challenged mice (n = 12–14/group).

Data are pooled from two (A and B) or three (D and E) repeats with n ≥ 5 mice/group. *p < 0.05 and **p < 0.01, Mann-Whitney test (A, B, and D) and log rank (Mantel-Cox) test (E).

highly purified D14PBS or D14LPS NK cells into naive mice and infected them intraperitoneally with *E. coli*, 2 days after transfer, and quantified bacterial burden and cell infiltrate. We observed reduced bacterial counts in the peritoneum of mice receiving D14LPS NK cells compared with those transferred with D14PBS NK cells (Figure 6A). This protective effect was accompanied by increased neutrophil recruitment to the peritoneum of mice that received D14LPS NK cells compared with D14PBS (Figure 6B). Taking advantage of a luminescent strain of *E. coli*, we assessed bacterial burden in parallel with survival. Interestingly, we observed significantly reduced luminescent signal 1 day post-

infection with *E. coli* in mice transferred with memory D14LPS NK cells compared with mice that received D14PBS NK cells (Figures 6C and 6D). Memory NK cell transfer also limited mortality in recipient mice, with a 53.8% survival rate compared with only 25% in recipients of control NK cells (Figure 6E). Our results thus show that memory-like NK cells have a beneficial effect during bacterial infection with *E. coli*. To determine whether methyltransferase-dependent memory properties of NK cells were playing a role in the protection against infection, we infected mice transferred with D14LPS NK cells treated with sinefungin. Strikingly, transfer of D14LPS-Snfg NK cells did not reduce bacterial counts or cause increased cellular infiltrate into the peritoneum, having effects comparable with those of D14PBS NK cells (Figures 6A and 6B). These results show that the protective effects of memory-like NK cells are fully dependent on methyltransferase-induced changes in NK cell properties. Interestingly, the protective effect seems to be specific, as we observed no differential *in vitro* response or *in vivo* protection when using an unrelated pathogen, *S. pneumoniae* (Figures S6A and S6B). Therefore, our results suggest that post-endotoxemia, memory-like NK cells play a beneficial role in bacterial infection by contributing to a reduction in bacterial burden through increased neutrophil infiltration. Additionally, memory-like NK cells have a certain degree of specificity to *E. coli* and not *S. pneumoniae*.

DISCUSSION

In this study we show that LPS-induced systemic inflammation drives the formation of memory-like NK cells that persist for at least 9 weeks after endotoxemia, even under the control of a suppressive environment in the spleen. We demonstrate that NK memory-like features are cell intrinsic and are acquired by cells present at the time of systemic inflammation that undergo proliferation. We further provide a molecular mechanism by which the memory is induced and/or maintained. We find that endotoxemia reveals a latent enhancer upstream of the *ifng* locus in NK cells, as seen by a significant increase in H3K4me1 levels, and that blocking methyltransferase activity can prevent acquisition of memory-like features. Finally, we show that endotoxemia-induced memory-like NK cells can protect against bacterial infection.

Previous studies have shown that memory NK cells were confined to specific sub-populations within the total NK cells pool (Hammer et al., 2018; Sun et al., 2009; Wight et al., 2018). Additionally, the memory subset of NK cells responds specifically to homologous and not heterologous challenge (Min-Oo and Lanier, 2014; Sun et al., 2009). A different situation occurs upon *in vitro* priming of NK cells with cytokines (IL-12, IL-15, and IL-18). NK cells retain memory-like features for several weeks after adoptive transfer into recipient mice, but these cells display increased IFN γ secretion capacity to several stimuli, such as cytokines and NK cell receptor ligation (Cooper et al., 2009), making them non-specific. Whether cytokine-induced memory is the same phenomenon as virus-induced memory remains to be determined. In our study we describe NK cells, which proliferate and display enhanced responsiveness to homologous re-stimulation without responding differently to secondary cytokine challenge or NK receptor triggering. In line with *in vitro* results, we find that

memory-like NK cells induced by systemic inflammation confer protection against *in vivo* challenge with *E. coli* but not *S. pneumoniae*. Our results thus show that memory-like NK cells induced by systemic inflammation are more similar to memory NK cells that develop following *in vivo* viral infection than *in vitro* generated cytokine-induced memory-like NK cells, showing increased IFN γ secretion and some degree of specificity.

It is worth mentioning that although the differences we observe in IFN γ response between naive and memory-like NK cells in our co-culture or transfer models are small (10%), we are analyzing the entire NK cell pool, which could account for the moderate extent of the observed differences, compared with previous studies in which only a sub-population of NK cells bearing memory was studied. Additionally, we acknowledge that we cannot fully exclude a contribution of ILC1 contamination in our NK preparations for the protection observed *in vivo*. We have, however, shown that the increased response *in vivo* and in our *in vitro* co-culture can be observed within the conventional NK cell population (CD49b+). Nevertheless, the bulk population memory-like responses we describe herein are clearly sufficient to elicit protection against bacterial infection upon adoptive transfer and to recruit more neutrophils.

In the context of systemic inflammation, our findings that NK cells acquire memory-like properties, leading to enhanced activation upon re-stimulation, are surprising because the consensus in literature is that NK cell functions are impaired during, and briefly following, acute episodes of sepsis (Guo et al., 2018). Indeed, when stimulated with cytokines, NK cells from acute phase sepsis patients or cecal ligation and puncture (CLP) mice were reported to have suppressed IFN γ production and cytotoxicity (Chiche et al., 2012; Jensen et al., 2018; Souza-Fonseca-Guimaraes et al., 2012b, 2012c; von Muller et al., 2007). However, few studies have investigated the post-acute long-term effects of systemic inflammation on NK cells and their cell-intrinsic activities independent of the immune environment. A recent report suggested that NK cell responsiveness was intact 7 days after bacterial and viral pneumonia, but activation during secondary infection was hampered by the immunosuppressive environment in the lungs (Roquilly et al., 2017). These results are similar to what we present here, where 2–9 weeks after endotoxemia, the environment restricts NK cell activation during re-stimulation, independently of their cell-intrinsic functions. As previously reported in CLP models (Benjamim et al., 2005; Cavassani et al., 2010; Delano et al., 2007; Nascimento et al., 2017; Wen et al., 2008), we also observed increased frequencies of Tregs and expansion of myeloid cells, suggesting that endotoxemia induces similar long-lasting consequences to CLP. Thus, our results provide new evidence on the persistent effect of systemic inflammation on NK cell status. We show that NK cell responsiveness to a second challenge with LPS is increased, in a cell-intrinsic manner, providing the first evidence of NK cell memory-like features following systemic inflammation.

Because of the nature of the LPS model we used in this study, a natural question is whether TLR4 is involved in endotoxemia-induced NK cell memory. Although LPS is the main ligand for TLR4, the role of this receptor for NK cells remains controversial. Although several studies described a role for TLRs in NK cell activation (Chalifour et al., 2004; Martinez et al., 2010), TLR4 was

shown to be dispensable for cell-intrinsic NK activation during endotoxemia *in vivo*, where NK cell response was dependent mostly on cytokines, including IFN β , IL-2, IL-15, IL-18, and IL-12 (Zanoni et al., 2013). In line with these results, we found that activation of NK cells is not dependent on TLR2 or TLR4 during both primary and secondary responses *in vivo*.

We believe that activation of NK cells during primary and secondary responses in our system would have to involve one or more NK cell receptors. Reports of NK cell memory to viruses and haptens show that specific receptors are involved in conferring a memory response (Cerwenka and Lanier, 2016). Recognition of the m157 glycoprotein of MCMV by Ly49H (Smith et al., 2002; Sun et al., 2009) and of haptens by Ly49C/I (O'Leary et al., 2006; Wight et al., 2018) in mice, and CMV peptides by the NKG2C receptor in humans (Hammer et al., 2018), substantiate the specificity of NK cells in both primary and recall responses. Receptor-driven NK cell memory was shown to be exquisitely specific and contained within a sub-population of cells carrying a given receptor (Hammer et al., 2018; O'Leary et al., 2006; Wight et al., 2018). Thus, the majority of memory NK cells described are characterized by a receptor, which defines memory sub-populations within the total pool. Although we have excluded the role of Ly49H and NKG2A/C/E, and we have not identified a specific receptor-defined sub-population responsible for mediating post-endotoxemia memory, the possibility remains that such a population exists.

Beyond the receptors at play in NK cell memory, the molecular mechanisms involved are just beginning to be uncovered. In mouse and human memory-like NK cells, changes in DNA methylation were shown to be correlated with differential transcriptional responses, suggesting that an epigenetic component could be involved (Lee et al., 2015; Luetke-Eversloh et al., 2014; Schlums et al., 2015). Recently, an extensive study of chromatin accessibility on MCMV-specific Ly49H memory NK cells was performed (Lau et al., 2018). These results highlighted that memory NK possess distinct chromatin accessibility states, similarly to memory CD8 cells. However, how this regulates gene expression remains unknown. In our study, we focused our work on the *ifng* locus as IFN γ expression, along with GM-CSF, were the ones differentially regulated between PBS-NK and LPS-NK cells. Furthermore, the upstream regions we studied were shown to be crucial for IFN γ expression and to have enhancer functions (Hattori et al., 2006). Here we show that memory-like NK cells acquire H3K4me1 at the –22 kb region, a modification most pronounced at 2 weeks after endotoxemia yet still present by 9 weeks, possibly because of a contraction of the memory population. Such, *de novo* marking of an enhancer was observed in memory CD8 T cells following LCMV infection (He et al., 2016) but has not been reported for NK cells. In addition, H3K4me1 enhancer marking in macrophages is retained upon signal termination and important for the augmented response upon re-stimulation (Ostuni et al., 2013). In combination with H3K4me1, other histone modifications, such as K3K27Ac and H3K27me3, correlate with either active or repressive gene activity (Bonn et al., 2012). In our study we find the –22 kb region associated with K3K27Ac and very low levels of H3K27me3, suggesting that when H3K4 becomes monomethylated, the enhancer will become active for

expression of IFN γ . Notably, other factors besides enhancer marking with K3K27Ac and H3K4me1, such as transcription factors, must be required to get full activation of IFN γ in memory-like NK cells. Indeed, IL-12+IL-18 did not differentially activate IFN γ in memory-like cells. Interestingly, *de novo* H3K4me1 marking in response to a stimulus, as we show in NK cells and others in macrophages, strongly suggests that the enhancer repertoire of a cell is not fixed upon terminal differentiation, can be expanded by external stimuli, and can be maintained for a memory response.

To date, evidence for NK cell memory to bacterial infection or sepsis is scarce. One report described a mouse model of BCG vaccination and *Mycobacterium tuberculosis* infection, showing an expansion of IFN γ +NKp46+CD27+ cells during re-infection and that transfer of these cells into naive mice could help control bacterial burden (Venkatasubramanian et al., 2017). Our results clearly demonstrate that systemic inflammation induced by LPS elicits memory-like NK cells, and these cells improve the response against *E. coli* infection when transferred into naive mice. Therefore, memory NK cells could be considered vaccination targets and efficacy readouts. This prospect is especially interesting given the important role NK cells play during bacterial infection and their potency in treating such diseases as cancer (Horowitz et al., 2012; Souza-Fonseca-Guimaraes et al., 2012a). In addition, our finding that NK cells' responsiveness to bacterial products is heightened, while that of the environment is suppressed, suggests that NK cells could be good targets for immunotherapy in order to modulate the post-sepsis immune system.

STAR★METHODS

Detailed methods are provided in the online version of this paper and include the following:

- KEY RESOURCES TABLE
- LEAD CONTACT AND MATERIALS AVAILABILITY
- EXPERIMENTAL MODEL AND SUBJECT DETAILS
- METHOD DETAILS
 - Cytometry staining protocols and analysis
 - NK cell enrichment and purification
 - Cell transfer and bacterial challenge experiments
 - NK cell culture and co-cultures
 - ChIP-qPCR assays
- QUANTIFICATION AND STATISTICAL ANALYSIS
- DATA AND CODE AVAILABILITY

SUPPLEMENTAL INFORMATION

Supplemental Information can be found online at <https://doi.org/10.1016/j.celrep.2019.11.043>.

ACKNOWLEDGMENTS

Work in the M.A.H. laboratory received financial support from Institut Pasteur and the French National Research Agency (ANR-EPIBACTIN). O.R. was supported by a stipend from the Pasteur – Paris University International PhD Program for part of this work. T.M.-N.C. is supported by a fellowship from the Foundation for Medical Research (Mariane Josso Prize). We would like to thank Olivier Dussurget and Emmanuel Lemichez for the kind gift of the luminescent *E. coli*, Thomas Kohler and Sven Hammerschmidt for the

S. pneumoniae strain, and Ignacio Santeccchia for technical assistance with *E. coli* culture.

AUTHOR CONTRIBUTIONS

O.R. coordinated the study. O.R., J.-M.C., and M.A.H. conceived and designed the study. O.R., C.C., T.M.-N.C., and C.F. performed experiments and analyzed data. O.R. and M.A.H. conceived and wrote the manuscript. J.-M.C. edited the manuscript. J.-M.C. and M.A.H. supervised the work.

DECLARATION OF INTERESTS

The authors declare no competing interests.

Received: March 28, 2019

Revised: September 6, 2019

Accepted: November 8, 2019

Published: December 17, 2019

REFERENCES

- Balasubramani, A., Winstead, C.J., Turner, H., Janowski, K.M., Harbour, S.N., Shibata, Y., Crawford, G.E., Hatton, R.D., and Weaver, C.T. (2014). Deletion of a conserved cis-element in the *lfn3* locus highlights the role of acute histone acetylation in modulating inducible gene transcription. *PLoS Genet.* *10*, e1003969.
- Batsché, E., Yaniv, M., and Muchardt, C. (2006). The human SWI/SNF subunit Brm is a regulator of alternative splicing. *Nat. Struct. Mol. Biol.* *13*, 22–29.
- Benjamim, C.F., Lundy, S.K., Lukacs, N.W., Hogaboam, C.M., and Kunkel, S.L. (2005). Reversal of long-term sepsis-induced immunosuppression by dendritic cells. *Blood* *105*, 3588–3595.
- Bonn, S., Zinnen, R.P., Girardot, C., Gustafson, E.H., Perez-Gonzalez, A., Delhomme, N., Ghavi-Helm, Y., Wilczyński, B., Riddell, A., and Furlong, E.E. (2012). Tissue-specific analysis of chromatin state identifies temporal signatures of enhancer activity during embryonic development. *Nat. Genet.* *44*, 148–156.
- Cavaillon, J.M., and Giamarellos-Bourboulis, E.J. (2019). Immunosuppression is inappropriately qualifying the immune status of septic and SIRS patients. *Shock* *52*, 307–317.
- Cavaillon, J.M., Adib-Conquy, M., Fitting, C., Adrie, C., and Payen, D. (2003). Cytokine cascade in sepsis. *Scand. J. Infect. Dis.* *35*, 535–544.
- Cavassani, K.A., Carson, W.F., 4th, Moreira, A.P., Wen, H., Schaller, M.A., Ishii, M., Lindell, D.M., Dou, Y., Lukacs, N.W., Keshamouni, V.G., et al. (2010). The post sepsis-induced expansion and enhanced function of regulatory T cells create an environment to potentiate tumor growth. *Blood* *115*, 4403–4411.
- Cerwenka, A., and Lanier, L.L. (2016). Natural killer cell memory in infection, inflammation and cancer. *Nat. Rev. Immunol.* *16*, 112–123.
- Chalifour, A., Jeannin, P., Gauchat, J.F., Blaecke, A., Malissard, M., N'Guyen, T., Thieblemont, N., and Delneste, Y. (2004). Direct bacterial protein PAMP recognition by human NK cells involves TLRs and triggers alpha-defensin production. *Blood* *104*, 1778–1783.
- Chiche, L., Forel, J.M., Thomas, G., Farnarier, C., Vely, F., Bléry, M., Papazian, L., and Vivier, E. (2011). The role of natural killer cells in sepsis. *J. Biomed. Biotechnol.* *2011*, 986491.
- Chiche, L., Forel, J.M., Thomas, G., Farnarier, C., Cognet, C., Guerville, C., Zandotti, C., Vély, F., Roch, A., Vivier, E., and Papazian, L. (2012). Interferon- γ production by natural killer cells and cytomegalovirus in critically ill patients. *Crit. Care Med.* *40*, 3162–3169.
- Cooper, M.A., Elliott, J.M., Keyel, P.A., Yang, L., Carrero, J.A., and Yokoyama, W.M. (2009). Cytokine-induced memory-like natural killer cells. *Proc. Natl. Acad. Sci. U S A* *106*, 1915–1919.
- Delano, M.J., Scumpia, P.O., Weinstein, J.S., Coco, D., Nagaraj, S., Kelly-Scumpia, K.M., O'Malley, K.A., Wynn, J.L., Antonenko, S., Al-Quran, S.Z., et al. (2007). MyD88-dependent expansion of an immature GR-1(+)CD11b(+)

- population induces T cell suppression and Th2 polarization in sepsis. *J. Exp. Med.* **204**, 1463–1474.
- Doye, A., Mettouchi, A., Bossis, G., Clément, R., Buisson-Touati, C., Flatau, G., Gagnoux, L., Piechaczyk, M., Boquet, P., and Lemichez, E. (2002). CNF1 exploits the ubiquitin-proteasome machinery to restrict Rho GTPase activation for bacterial host cell invasion. *Cell* **111**, 553–564.
- Ganal, S.C., Sanos, S.L., Kallfass, C., Oberle, K., Johner, C., Kirschning, C., Lienenklaus, S., Weiss, S., Staeheli, P., Aichele, P., and Diefenbach, A. (2012). Priming of natural killer cells by nonmucosal mononuclear phagocytes requires instructive signals from commensal microbiota. *Immunity* **37**, 171–186.
- Gao, Y., Souza-Fonseca-Guimaraes, F., Bald, T., Ng, S.S., Young, A., Ngiow, S.F., Rautela, J., Straube, J., Waddell, N., Blake, S.J., et al. (2017). Tumor immunoevasion by the conversion of effector NK cells into type 1 innate lymphoid cells. *Nat. Immunol.* **18**, 1004–1015.
- Geary, C.D., and Sun, J.C. (2017). Memory responses of natural killer cells. *Semin. Immunol.* **37**, 11–19.
- Guo, Y., Patil, N.K., Luan, L., Bohannon, J.K., and Sherwood, E.R. (2018). The biology of natural killer cells during sepsis. *Immunology* **153**, 190–202.
- Hammer, Q., Rückert, T., Borst, E.M., Dunst, J., Haubner, A., Durek, P., Heinrich, F., Gasparoni, G., Babic, M., Tomic, A., et al. (2018). Peptide-specific recognition of human cytomegalovirus strains controls adaptive natural killer cells. *Nat. Immunol.* **19**, 453–463.
- Hatton, R.D., Harrington, L.E., Luther, R.J., Wakefield, T., Janowski, K.M., Oliver, J.R., Lallone, R.L., Murphy, K.M., and Weaver, C.T. (2006). A distal conserved sequence element controls *Irfng* gene expression by T cells and NK cells. *Immunity* **25**, 717–729.
- He, B., Xing, S., Chen, C., Gao, P., Teng, L., Shan, Q., Gullicksrud, J.A., Martin, M.D., Yu, S., Harty, J.T., et al. (2016). CD8⁺ T cells utilize highly dynamic enhancer repertoires and regulatory circuitry in response to infections. *Immunity* **45**, 1341–1354.
- Horowitz, A., Stegmann, K.A., and Riley, E.M. (2012). Activation of natural killer cells during microbial infections. *Front. Immunol.* **2**, 88.
- Jensen, I.J., Winborn, C.S., Fosdick, M.G., Shao, P., Tremblay, M.M., Shan, Q., Tripathy, S.K., Snyder, C.M., Xue, H.H., Griffith, T.S., et al. (2018). Polymicrobial sepsis influences NK-cell-mediated immunity by diminishing NK-cell-intrinsic receptor-mediated effector responses to viral ligands or infections. *PLoS Pathog.* **14**, e1007405.
- Lau, C.M., Adams, N.M., Geary, C.D., Weizman, O.E., Rapp, M., Pritykin, Y., Leslie, C.S., and Sun, J.C. (2018). Epigenetic control of innate and adaptive immune memory. *Nat. Immunol.* **19**, 963–972.
- Lee, J., Zhang, T., Hwang, I., Kim, A., Nitschke, L., Kim, M., Scott, J.M., Kamimura, Y., Lanier, L.L., and Kim, S. (2015). Epigenetic modification and antibody-dependent expansion of memory-like NK cells in human cytomegalovirus-infected individuals. *Immunity* **42**, 431–442.
- Lopez-Vergès, S., Milush, J.M., Schwartz, B.S., Pando, M.J., Jarjoura, J., York, V.A., Houchins, J.P., Miller, S., Kang, S.M., Norris, P.J., et al. (2011). Expansion of a unique CD57⁺NKG2Chi natural killer cell subset during acute human cytomegalovirus infection. *Proc. Natl. Acad. Sci. U S A* **108**, 14725–14732.
- Luetke-Eversloh, M., Hammer, Q., Durek, P., Nordström, K., Gasparoni, G., Pink, M., Hamann, A., Walter, J., Chang, H.D., Dong, J., and Romagnani, C. (2014). Human cytomegalovirus drives epigenetic imprinting of the *IFNG* locus in NKG2Chi natural killer cells. *PLoS Pathog.* **10**, e1004441.
- Martinez, J., Huang, X., and Yang, Y. (2010). Direct TLR2 signaling is critical for NK cell activation and function in response to vaccinia viral infection. *PLoS Pathog.* **6**, e1000811.
- Min-Oo, G., and Lanier, L.L. (2014). Cytomegalovirus generates long-lived antigen-specific NK cells with diminished bystander activation to heterologous infection. *J. Exp. Med.* **211**, 2669–2680.
- Nascimento, D.C., Melo, P.H., Piñeros, A.R., Ferreira, R.G., Colón, D.F., Donate, P.B., Castanheira, F.V., Gozzi, A., Czaikoski, P.G., Niedbala, W., et al. (2017). IL-33 contributes to sepsis-induced long-term immunosuppression by expanding the regulatory T cell population. *Nat. Commun.* **8**, 14919.
- Netea, M.G., Quintin, J., and van der Meer, J.W. (2011). Trained immunity: a memory for innate host defense. *Cell Host Microbe* **9**, 355–361.
- Netea, M.G., Joosten, L.A., Latz, E., Mills, K.H., Natoli, G., Stunnenberg, H.G., O'Neill, L.A., and Xavier, R.J. (2016). Trained immunity: A program of innate immune memory in health and disease. *Science* **352**, aaf1098.
- O'Leary, J.G., Goodarzi, M., Drayton, D.L., and von Andrian, U.H. (2006). T cell- and B cell-independent adaptive immunity mediated by natural killer cells. *Nat. Immunol.* **7**, 507–516.
- Ostuni, R., Piccolo, V., Barozzi, I., Polletti, S., Termanini, A., Bonifacio, S., Curina, A., Prosperini, E., Ghisletti, S., and Natoli, G. (2013). Latent enhancers activated by stimulation in differentiated cells. *Cell* **152**, 157–171.
- Rasid, O., Ciulean, I.S., Fitting, C., Doyen, N., and Cavallion, J.M. (2016). Local microenvironment controls the compartmentalization of NK cell responses during systemic inflammation in mice. *J. Immunol.* **197**, 2444–2454.
- Roquilly, A., McWilliam, H.E.G., Jacqueline, C., Tian, Z., Cinotti, R., Rimbart, M., Wakim, L., Caminschi, I., Lahoud, M.H., Belz, G.T., et al. (2017). Local modulation of antigen-presenting cell development after resolution of pneumonia induces long-term susceptibility to secondary infections. *Immunity* **47**, 135–147.e5.
- Saeed, S., Quintin, J., Kerstens, H.H., Rao, N.A., Aghajani-farah, A., Matarese, F., Cheng, S.C., Ratter, J., Berentsen, K., van der Ent, M.A., et al. (2014). Epigenetic programming of monocyte-to-macrophage differentiation and trained innate immunity. *Science* **345**, 1251086.
- Saleh, M., Abdullah, M.R., Schulz, C., Kohler, T., Pribyl, T., Jensch, I., and Hammerschmidt, S. (2014). Following in real time the impact of pneumococcal virulence factors in an acute mouse pneumonia model using bioluminescent bacteria. *J. Vis. Exp.* **84**, e51174.
- Sasaki, K., Doi, S., Nakashima, A., Irifuku, T., Yamada, K., Kokoroishi, K., Ueno, T., Doi, T., Hida, E., Arihiro, K., et al. (2016). Inhibition of SET domain-containing lysine methyltransferase 7/9 ameliorates renal fibrosis. *J. Am. Soc. Nephrol.* **27**, 203–215.
- Schlums, H., Cichocki, F., Tesi, B., Theorell, J., Beziat, V., Holmes, T.D., Han, H., Chiang, S.C., Foley, B., Mattsson, K., et al. (2015). Cytomegalovirus infection drives adaptive epigenetic diversification of NK cells with altered signaling and effector function. *Immunity* **42**, 443–456.
- Shankar-Hari, M., and Rubenfeld, G.D. (2016). Understanding long-term outcomes following sepsis: implications and challenges. *Curr. Infect. Dis. Rep.* **18**, 37.
- Smith, H.R., Heusel, J.W., Mehta, I.K., Kim, S., Dorner, B.G., Naidenko, O.V., Iizuka, K., Furukawa, H., Beckman, D.L., Pingel, J.T., et al. (2002). Recognition of a virus-encoded ligand by a natural killer cell activation receptor. *Proc. Natl. Acad. Sci. U S A* **99**, 8826–8831.
- Souza-Fonseca-Guimaraes, F., Adib-Conquy, M., and Cavallion, J.M. (2012a). Natural killer (NK) cells in antibacterial innate immunity: angels or devils? *Mol. Med.* **18**, 270–285.
- Souza-Fonseca-Guimaraes, F., Parlato, M., Fitting, C., Cavallion, J.M., and Adib-Conquy, M. (2012b). NK cell tolerance to TLR agonists mediated by regulatory T cells after polymicrobial sepsis. *J. Immunol.* **188**, 5850–5858.
- Souza-Fonseca-Guimaraes, F., Parlato, M., Philippart, F., Misset, B., Cavallion, J.M., and Adib-Conquy, M.; Captain Study Group (2012c). Toll-like receptors expression and interferon- γ production by NK cells in human sepsis. *Crit. Care* **16**, R206.
- Sun, J.C., Beilke, J.N., and Lanier, L.L. (2009). Adaptive immune features of natural killer cells. *Nature* **457**, 557–561.
- Sun, J.C., Ugolini, S., and Vivier, E. (2014). Immunological memory within the innate immune system. *EMBO J.* **33**, 1295–1303.
- Tesi, B., Schlums, H., Cichocki, F., and Bryceson, Y.T. (2016). Epigenetic regulation of adaptive NK cell diversification. *Trends Immunol.* **37**, 451–461.
- Venkatasubramanian, S., Cheekatla, S., Paidipally, P., Tripathi, D., Welch, E., Tvinnereim, A.R., Nurieva, R., and Vankayalapati, R. (2017). IL-21-dependent expansion of memory-like NK cells enhances protective immune responses against *Mycobacterium tuberculosis*. *Mucosal Immunol.* **10**, 1031–1042.

- Vivier, E., Tomasello, E., Baratin, M., Walzer, T., and Ugolini, S. (2008). Functions of natural killer cells. *Nat. Immunol.* **9**, 503–510.
- von Muller, L., Klemm, A., Durmus, N., Weiss, M., Suger-Wiedeck, H., Schneider, M., Hampf, W., and Mertens, T. (2007). Cellular immunity and active human cytomegalovirus infection in patients with septic shock. *J. Infect. Dis.* **196**, 1288–1295.
- Wen, H., Dou, Y., Hogaboam, C.M., and Kunkel, S.L. (2008). Epigenetic regulation of dendritic cell-derived interleukin-12 facilitates immunosuppression after a severe innate immune response. *Blood* **111**, 1797–1804.
- Wight, A., Mahmoud, A.B., Scur, M., Tu, M.M., Rahim, M.M.A., Sad, S., and Makrigiannis, A.P. (2018). Critical role for the Ly49 family of class I MHC receptors in adaptive natural killer cell responses. *Proc. Natl. Acad. Sci. USA* **115**, 11579–11584.
- Winson, M.K., Swift, S., Hill, P.J., Sims, C.M., Griesmayr, G., Bycroft, B.W., Williams, P., and Stewart, G.S.A.B. (1998). Engineering the luxCDABE genes from *Photobacterium luminescens* to provide a bioluminescent reporter for constitutive and promoter probe plasmids and mini-Tn5 constructs. *FEMS Microbiol. Lett.* **163**, 193–202.
- Zanoni, I., Spreafico, R., Bodio, C., Di Gioia, M., Cigni, C., Broggi, A., Gorletta, T., Caccia, M., Chirico, G., Sironi, L., et al. (2013). IL-15 cis presentation is required for optimal NK cell activation in lipopolysaccharide-mediated inflammatory conditions. *Cell Rep.* **4**, 1235–1249.

STAR★METHODS

KEY RESOURCES TABLE

REAGENT or RESOURCE	SOURCE	IDENTIFIER
Antibodies		
CD16/CD32 mouse	BD Biosciences	Cat# 553142, RRID:AB_394657
NK1.1 (PK136), BV421	BioLegend	Cat# 108732, RRID:AB_2562218
CD3e (145-2C11), PE-Cy7	Thermo Fisher Scientific	Cat# 25-0031-82, RRID:AB_469572
CD3e (145-2C11), PerCP-Cy5.5	Thermo Fisher Scientific	Cat# 45-0031-82, RRID:AB_1107000
CD49b (DX5), PE	Thermo Fisher Scientific	Cat# 12-5971-82, RRID:AB_466073
CD69 (H1.2F3), FITC	Thermo Fisher Scientific	Cat# 11-0691-82, RRID:AB_465119
Ly6C (HK1.4), PE-Cy7	BioLegend	Cat# 128017, RRID:AB_1732093
CD11b (M1/70), eF450	Thermo Fisher Scientific	Cat# 48-0112-82, RRID:AB_1582236
Ly6G (1A8-Ly6g), FITC	Thermo Fisher Scientific	Cat# 11-9668-82, RRID:AB_2572532
CD11c (HL3), APC	BD Biosciences	Cat# 550261, RRID:AB_398460
CD45.1 (A20), PE	Thermo Fisher Scientific	Cat# 12-0453-82, RRID:AB_465675
CD45.1 (A20), PE-Cy7	Thermo Fisher Scientific	Cat# 25-0453-82, RRID:AB_469629
CD45.2 (104), FITC	Thermo Fisher Scientific	Cat# 11-0454-82, RRID:AB_465061
CD45.2 (104), PE-Cy7	Thermo Fisher Scientific	Cat# 25-0454-82, RRID:AB_2573350
foxp3 (FJK-16 s), PE	Thermo Fisher Scientific	Cat# 12-5773-82, RRID:AB_465936
IFN γ (XMG1.2), APC	Thermo Fisher Scientific	Cat# 17-7311-82, RRID:AB_469504
CD4 (RM4-5), PerCP-Cy5.5	Thermo Fisher Scientific	Cat# 45-0042-82, RRID:AB_1107001
Ly49H (REA241), PE	Miltenyi Biotec	Cat# 130-102-704, RRID:AB_2652766
Ly49F (HBF-719), PE	Miltenyi Biotec	Cat# 130-104-292, RRID:AB_2652744
Ly49D (4E5), APC	Miltenyi Biotec	Cat# 130-103-313, RRID:AB_2652713
Ly49C/1 (REA253), APC	Miltenyi Biotec	Cat# 130-103-394, RRID:AB_2652705
NKG2A/C/E (20d5), APC	Miltenyi Biotec	Cat# 130-105-621, RRID:AB_2653007
CD314/NKG2D (CX5), PE	Miltenyi Biotec	Cat# 130-103-367, RRID:AB_2657375
H3K27ac Rabbit polyclonal antibody	Abcam	Cat# ab4729, RRID:AB_2118291
H3K27me3 Rabbit polyclonal antibody	Abcam	Cat# ab6002, RRID:AB_305237
H3K4me1 Rabbit polyclonal antibody	Diagenode	Cat# C15410194, RRID:AB_2637078
H3K4me3 Rabbit polyclonal antibody	Diagenode	Cat# pAb-003-050, RRID:AB_2616052
H3 Rabbit polyclonal antibody	Abcam	Cat# ab1791, RRID:AB_302613
Rabbit IgG, polyclonal - Isotype Control	Abcam	Cat# ab37415, RRID:AB_2631996
Bacterial and Virus Strains		
<i>Escherichia coli</i> Background strain 58A1	Gift from O. Dussurget and E. Lemichez (Doye et al., 2002)	N/A
<i>Streptococcus pneumoniae</i> Tigr4	Gift from Thomas Kohler and Sven Hammerschmidt (Saleh et al., 2014)	N/A
Chemicals, Peptides, and Recombinant Proteins		
Recombinant Mouse IL-18	MBL	Cat#B002-5
Mouse IL-12	Miltenyi Biotec	Cat#130-096-708
Mouse IL-15	Miltenyi Biotec	Cat#130-094-072
Sinefungin, methyltransferase inhibitor	Abcam	Cat#ab144518
Lipopolysaccharides from <i>Escherichia coli</i> O111:B4	Sigma Aldrich	Cat#L2630-25MG
Critical Commercial Assays		
NK Cell Isolation Kit, mouse	Miltenyi Biotec	Cat# 130-115-818
Mouse IFN-gamma DuoSet ELISA	Bio-Techne	Cat# DY485
Mouse GM-CSF DuoSet ELISA	Bio-Techne	Cat# DY415

(Continued on next page)

Continued

REAGENT or RESOURCE	SOURCE	IDENTIFIER
MagniSort Mouse NK cell Enrichment Kit	Thermo Fisher Scientific	Cat# 8804-6828-74, RRID:AB_2575268
Experimental Models: Organisms/Strains		
Mouse C57BL/6J	Janvier Labs	N/A
Mouse C57BL/6J CD45.1	Institut Pasteur	N/A
Mouse C57BL/6J CD45.1/2	Institut Pasteur	N/A
Software and Algorithms		
Flow Jo-v10	Flow Jo, LLC	https://www.flowjo.com
Prism 7	Prism-Graphpad	https://www.graphpad.com

LEAD CONTACT AND MATERIALS AVAILABILITY

Further information and requests for resources and reagents should be directed to and will be fulfilled by the Lead Contact, Melanie Anne Hamon (melanie.hamon@pasteur.fr). This study did not generate new unique reagents or materials.

EXPERIMENTAL MODEL AND SUBJECT DETAILS

All protocols for animal experiments were reviewed and approved by the CETEA (Comité d'Ethique pour l'Expérimentation Animale - Ethics Committee for Animal Experimentation) of the Institut Pasteur under approval number 2016-003 and were performed in accordance with national laws and institutional guidelines for animal care and use. CD45.1, CD45.2 and CD45.1/2 mice, males of 8 to 12 weeks were purchased from Janvier (France) or bred at the Institut Pasteur animal facility. For endotoxemia, mice were injected intraperitoneally with a single dose of conventional LPS from *E. coli* O111:B4, 10 mg/kg in a 200 μ L volume of PBS. Control mice received just PBS injections. Animals were monitored daily for the first 5 days and then weekly for the duration of the experiment. Animals were sacrificed in the event they lost more than 20% of weight as a result of endotoxemia (mortality was usually below 10% at this dose of LPS). A clinical score was used to assess progression of mice throughout endotoxemia, representing the sum of the following scores: 0 – no clinical signs; 1 – hypoactivity; 1 – ruffled fur; 2 – hunched posture; 2 – diarrhea; 3 – prostration. For histone methyltransferase inhibition experiments, mice were treated at day 2 after PBS/LPS injection with saline or Sinefungin (10 mg/kg, i.p. in a 200 μ L volume of saline).

METHOD DETAILS**Cytometry staining protocols and analysis**

Single cell suspensions from spleens were counted and prepared for surface staining in 96 well plates. Unspecific binding was first blocked by incubation with anti-mouse CD16/CD32 for 10 minutes before addition of surface labeling antibodies for another 45 minutes, in 0,5% FCS at 4°C. Cells were washed twice in PBS in preparation for viability staining using fixable viability dye (eFluor780, ebioscience) for 5 minutes at 4°C. Cells were washed twice in 0,5% FCS and fixed using commercial fixation buffer (Biolegend). For intracellular cytokine and Foxp3 staining, cells were permeabilized and washed with buffers from commercial kits (Inside Stain Kit, Miltenyi Biotec and Foxp3 / Transcription Factor Fixation/Permeabilization Concentrate and Diluent, eBioscience, respectively). Following permeabilization and washing, cells were stained with respective antibodies in 0,5% FCS for 30 minutes at 4°C and after a final washing suspended in buffer for FACS analysis. Sample acquisition was performed on a MACSQuant flow-cytometer (Miltenyi Biotec) and analysis was done using FlowJo Software (TreeStar).

NK cell enrichment and purification

Splenocytes obtained by mechanical dissociation of spleens were passed successively through 100 μ m, 70 μ m and 30 μ m strainers (Miltenyi Biotec) and counted before use for downstream applications. NK cells were enriched from splenocyte suspensions using negative enrichment kits (eBioscience) according to manufacturer's protocol but combined with separation over magnetic columns (LS columns, Miltenyi Biotec) and were routinely brought to 80% purity. For some *in vitro* stimulations and transfers of cells before bacterial challenge, enriched NK cells were re-purified using mouse NK cell purification kits (Miltenyi Biotec) according to manufacturer's instructions to reach purities of approximately 98%.

Cell transfer and bacterial challenge experiments

Enriched NK cells from CD45.1, CD45.2 or CD45.1/2 mice were transferred i.v. into recipient congenic mice ($0,75-1 \times 10^6$ cells/recipient) in 100 μ L of PBS. For forward transfers, NK cells were transferred into congenic naive mice 1 day before LPS challenge. At 6 hours after PBS or LPS injection, single cell suspensions were obtained from spleen of recipient mice and flow cytometric analysis

was performed. For pre-/post-transfer experiments, CD45.1 NK cells were pre-transferred into CD45.1/2 mice 1 day before endotoxemia induction and naive CD45.2 NK cells were post-transferred 7 days after. At day 14 after endotoxemia, mice were re-challenged with PBS/LPS and NK cell responses were assessed by flow cytometry as described above. For proliferation assessment experiments, enriched NK cells were stained with CFSE 2,5 μ M in PBS for 10 minutes, before blocking in FCS and extensively washed with PBS before transfer into congenic mice, 1 day before endotoxemia induction. For bacterial challenge experiments 10^5 highly purified NK cells from D13PBS or LPS mice were transferred to naive 2 days before challenge with $1\text{--}2 \times 10^7$ *E. coli* intraperitoneally or 5×10^6 *S. pneumoniae* intravenously, serotype 4 (Thomas Kohler, Universität Greifswald). For bacterial inoculums, experimental starters were grown to midlog phase in Luria-Bertani (BD) supplemented with streptomycin (200 μ g/ml) and ampicillin (50 μ g/ml) for *E. coli* or Todd-Hewitt (BD) broth supplemented with 50mM HEPES (Sigma) (TH+H) at 37°C with 5% CO₂ for *S. pneumoniae*. Bacterial cultures were washed thrice in PBS, and concentrated in 1mL PBS prior to dilution at the desired CFU/mL for mouse infection. Luminescent *E. coli* was made by insertion of pLac-luxABCDE plasmid pSB417 (Winson et al., 1998) into *E. coli* strain 58A1 (Doye et al., 2002). Peritoneal lavages from were serially diluted and plated for CFU counts and cells were stained as above.

NK cell culture and co-cultures

Purified NK cells were cultured at 1×10^6 cells/ml in 200 μ L RPMI 1640 (GIBCO) supplemented with 10% FCS and Penicillin-Streptomycin (GIBCO) respectively in 96 well round-bottom plates (Nunc). Cells were either left unstimulated or activated with conventional LPS from *E. coli* O111:B4 at 100ng/ml or various cytokine cocktails composed of IL-15, IL-12 and IL-18 at a dose of 10ng/ml each. NK cell were additionally stimulated with LPS + cytokine cocktails. After 20 hours of culture, cells were collected for intracellular cytokine staining by flow cytometry and culture supernatants were collected and stored at -20°C for cytokine assays performed by ELISA according to manufacturer's instructions (DuoSet, R&D Systems).

ChIP-qPCR assays

ChIP was performed as described before by Batsché et al. (2006) with some modifications. NK cells were fixed in 1% formaldehyde (8 min, room temperature), and the reaction was stopped by the addition of glycine at the final concentration of 0,125 M. After two washes in PBS, cells were resuspended in 0.25% Triton X-100, 10 mM Tris-HCl (pH 8), 10 mM EDTA, 0.5 mM EGTA and proteases inhibitors; the soluble fraction was eliminated by centrifugation; and chromatin was extracted with 250 mM NaCl, 50 mM Tris-HCl (pH 8), 1 mM EDTA, 0.5 mM EGTA and proteases inhibitors cocktail for 30 min on ice. Chromatin was resuspended in 1% SDS, 10 mM Tris-HCl (pH 8), 1 mM EDTA, 0.5 mM EGTA and proteases inhibitors cocktail; and sonicated during 8 cycles using Diagenode Bioruptor Pico (15 s on, 30 s off). DNA fragment size (< 1 kb) was verified by agarose gel electrophoresis. ChIP was performed using H3, H3K4me3, H3K27ac, H3K27me3, H3K4me1 antibodies and nonimmune IgG (negative control antibody), chromatin extracted from 3×10^6 NK cells per condition was used. Chromatin was diluted 10 times in 0.6% Triton X-100, 0.06% sodium deoxycholate (NaDOC), 150 mM NaCl, 12 mM Tris-HCl, 1 mM EDTA, 0.5 mM EGTA and proteases inhibitors cocktail. For 6 hours, the different antibodies were previously incubated at 4°C with protein G-coated magnetic beads (DiaMag, Diagenode), protease inhibitor cocktail and 0.1% BSA. Chromatin was incubated overnight at 4°C with each antibody/protein G-coated magnetic beads. Immunocomplexes were washed with 1 x buffer 1 (1% Triton X-100, 0.1% NaDOC, 150 mM NaCl, 10 mM Tris-HCl (pH 8)), 1 x buffer 2 (0.5% NP-40, 0.5% Triton X-100, 0.5 NaDOC, 150 mM NaCl, 10 mM Tris-HCl (pH 8)), 1 x buffer 3 (0.7% Triton X-100, 0.1% NaDOC, 250 mM NaCl, 10 mM Tris-HCl (pH 8)) 1 x buffer 4 (0.5% NP-40, 0.5% NaDOC, 250 mM LiCl, 20 mM Tris-HCl (pH 8), 1 mM EDTA), 1 x buffer 5 (0,1% NP-40, 150 mM NaCl, 20 mM Tris-HCl (pH 8), 1 mM EDTA) and 1 x buffer 6 (20mM Tris-HCl (pH 8), 1 mM EDTA) . Beads were eluted in water containing 10% Chelex and reverse cross-linked by boiling for 10 min, incubating with RNase for 10 min at room temperature, then with proteinase K for 20 min at 55°C and reboiling for 10 min. DNA fragment were purified by Phenol Chloroform extraction.

Amplifications (40 cycles) were performed using quantitative real-time PCR using iTaq™ Universal Syber Green Supermix (BIORAD) on a CFX384 Touch Real-Time PCR system (BIORAD). qPCR efficiency (E) was determined for the ChIP primers with a dilution series of genomic mouse DNA. The threshold cycles (Ct values) were recordered from the exponential phase of the qPCR for IP and input DNA for each primer pair. The relative amount of immunoprecipitated DNA was compared to input DNA for the control regions (% of recovery) using the following formula: % recovery = $E^{-((Ct(1\% \text{ input}) - \text{Log}_2(\text{input dilution})) - Ct(\text{IP}))} \times 100$. Antibodies ChIP-grade and ChIP primers sequences are provided in Table S1

QUANTIFICATION AND STATISTICAL ANALYSIS

Statistical significance was tested using Prism 7.0 Software (GraphPad). Mann Whitney test was used for single comparisons, Wilcoxon paired test for paired comparison of samples in the same mouse in transfer experiments or in the same well for co-culture experiments and Log-rank (Mantel-Cox) test for survival curves. Unless otherwise specified in figure legends, error bars in all figures represent SEM, with the midlines representing the mean value.

DATA AND CODE AVAILABILITY

This study did not generate any unique datasets or code.